Trichromatic Reflectance Capture Using a Tunable Light Source: Setup, Characterization and Reflectance Estimation

Tejas Madan Tanksale and Philipp Urban
Fraunhofer Institute for Computer Graphics Research IGD,
Fraunhoferstr. 5, 64283 Darmstadt, Germany

Abstract

A research project is underway to develop a gonio imager particularly dedicated to sample the Bidirectional Reflectance Distribution Function (BRDF) of materials and material compositions employed and created by multimaterial 3D printers. It comprises an almost colorimetric RGB camera and a spectrally tunable light source. In this paper, we investigate an important part of this system, particularly the approach to estimate reflectances from RGB values acquired under multiple illuminants. We first characterize the system by estimating the spectral sensitivities of the camera. Then, we use the sensitivities, a set of illuminants produced by the tunable light source and the corresponding sensor responses to estimate reflectances. For evaluating this approach, we measure the Neugebauer primary reflectances of a polyjet printer employing highly translucent photo-polymer printing materials colored in cyan, magenta, yellow and white. Spectral and colorimetric deviations to spectroradiometric comparison measurements (average 0.67 CIEDE2000 units / 0.0286 spectral RMS) are within the inter-instrument variability of hand-held spectrophotometers used in graphic arts for prints on paper.

Introduction and Motivation

Today's high-resolution 3D printers – particularly polyjetting printers – can combine multiple colored materials on a droplet-basis in a single object enabling the reproduction of various appearance attributes such as color, gloss or goniochromatic effects. This is possible by arranging printing materials in halftone patterns to create various color shades, printing varnish halftones to create multiple gloss shades or by printing microfacets on top of the surface to produce anisotrpopic reflectance.

The presented work is motivated by the challenging task to spectrally modeling such printers particularly to accurately measure the reflectances of printed samples used to develop and to fit spectral printer models.

Even if we consider the simple case of flat printed samples and are interested only in a 45/0 measurement geometry, measurements made by spectrophotometers from graphic arts are biased towards lower reflectances because of the high translucency of the used photo-polymeric printing materials as explained in detail in [1]. In this reference, a measurement methodology is presented to obtain CIELAB values employing an almost colorimetric camera, highly-uniform broadband illumination simulating CIED50, flat-fielding to account for inhomogeneous light intensities and a polynomial approach to map RGB values to CIEXYZ. As long as the number of printing materials is low, these measurements can be used in a full empirical printer model (regular sampling of the colorant space and interpolating intermediate colors), e.g. to create ICC profiles. Figure 1 shows a target to colorimetrically model a CMYW 3D printer with 512 patches.

If the number of materials increases, full empirical models are impractical because the number of measurements increases exponentially with the number of materials. In this case, physical models, e.g. based on the radiative transfer theory, or partly empirical models are necessary requiring accurate bidirectional reflectance measurements of selected print samples. For this, a spectral acquisition system is required, which allows us to capture reflectance data for the whole printed target employing arbitrary bidirectional measurement geometries. Furthermore, the target must be illuminated very uniformly, because flat-fielding cannot correct errors caused by subsurface light transport between the target's patches.

We are in the process of developing a gonio-imager to sample the *Bidirectional Reflectance Distribution Function* (BRDF) of printed samples. Instead of using a spectral camera, it contains a commercially available spectrally tunable light source and an almost colorimetric RGB camera. The light source employs 22 different LEDs (20 spectrally narrowband LEDs covering the whole visible wavelength range and two white light LEDs) and an internal spectroradiometer ensuring a stable spectral power distribution (SPD). Furthermore, the actual SPD of the light source during the capturing process is recorded and is available for reflectance estimation. Capturing a white reference for canceling out the illuminant is not required in this setup. Both the camera and the tunable light source can be controlled by an Application Programming Interface (API) allowing a fully automatic multichannel acquisition. In this way, both the intensity of the illuminant or the exposure time can be adjusted to capture High Dynamic Range (HDR) images, which is necessary to measure the specular lobe.

Another interesting property is the combination of an almost colorimetric camera with a spectrally tunable light source: Accurate CIEXYZ data of samples for a particular illuminant can be captured in a single shot for each geometry by simply adjusting the tunable light source to the desired SPD. To reduce measurement time, a sparse spectral reflectance sampling and a dense CIEXYZ sampling can be performed. A dense spectral representation of the BRDF can then be computed from these data subject to a high colorimetric accuracy for the considered illuminant. A similar strategy was proposed in the scope of 2D spectral imaging [16, 17].

In this work, we are investigating the spectral accuracy of this setup. This includes measuring the spectral sensitivities of the camera and estimating reflectance from multi-illuminant RGB acquisitions. Since the mechanical setup is still under construc-

tion, all measurements conducted in this work are restricted to the 0/45 geometry.

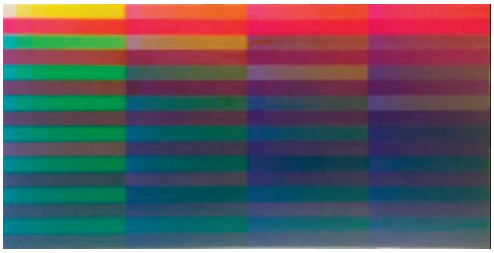

Figure 1: 3D printed target used to characterize a printing system.

Related Work

For the sake of simplicity, we use a vector representation of spectra and sensitivities, i.e. each wavelength-dependent quantity $X(\lambda)$ is equidistantly sampled in the sensitivity range Ω of the camera resulting in $\mathbf{x} = (X(\lambda_1), \ldots, X(\lambda_n))^T$, where $[\lambda_1, \lambda_n] = \Omega$ and $\forall i, j < n : \lambda_{i+1} - \lambda_i = \lambda_{j+1} - \lambda_j$.

Assuming linearity, the m-dimensional column vector of camera responses $\mathbf{c}$ is modeled as follows:

$$\mathbf{c} = \mathbf{S}D(\mathbf{i})\mathbf{r} + \varepsilon \tag{1}$$

where $\mathbf{S}$ is the $m \times n$ dimensional matrix with the camera sensitivity as row vectors, $\mathbf{i}$ is the illuminant, D is an operator that transforms a vector into a diagonal matrix with the vector entries in the diagonal, $\mathbf{r}$ is the spectral reflectance and ε represents noise. The internal spectroradiometer of the tuneable light source gives us $\mathbf{i}$. To estimate the reflectance $\mathbf{r}$, we need to accurately know the camera's spectral sensitivities $\mathbf{S}$. These are measured by employing again the spectrally tuneable light source.

The camera sensitivities can be obtained in two possible ways: directly measuring them employing a monochromator, or estimating them from known stimuli. The monochromator approach is straightforward [18] but requires additional expensive equipment. The second way includes various approaches that use *a priori* knowledge to solve Eq. (1) with respect to the sensitivities, e.g. Linear- or quadratic programming [11, 7], projection onto convex sets [19, 20], evolutionary algorithms [5] or low-dimensional models of spectral sensitivities [26, 10]. For creating the required stimuli typically a reflectance target illuminated by a single light source is used. To increase the dimensionality of the set of stimuli, multiple captures of a spectrally measured target under different known LED illuminants were proposed [23]. Also approaches that do not require the knowledge of the illuminant's spectral power distribution are proposed employing a fluorescent chart [9].

Solving Eq. (1) with respect to the reflectance is referred to reflectance estimation. This is mostly an ill-posed problem since the number of camera responses is smaller than the number of spectral components. Therefore, *a priori* knowledge on spectral reflectances is used to obtain reasonable results: Maloney et al. used a low-dimensional linear reflectance model [13], other researchers picked the smoothest reflectance [12, 3, 14], principal component analysis and Wiener estimation [21], adaptive principal component analysis [25], extend the linear reflectance model to manifolds [4] or use kernel-based methods [6]. For capturing images, methods were proposed that include *a priori* knowledge on inter-pixel correlation [15, 22] and the point spread function of the acquisition system [8].

Methodology

Our setup consists of the Image Engineering CAL1 spectrally-tunable light source employing 22 LEDs (Figure 2 shows the LEDs' spectral power distributions) and a Canon 5D Mark III DSLR camera. Camera and light source are arranged in a 0/45 measurement geometry with approx. 70cm distance from the sample plane as shown in Figure 3. The exposure time for each illuminant is set to six seconds to exploit the whole bit-depth of the camera considering the low intensity of the stimuli caused by the narrow-band SPDs of most of the LEDs as well as the distance between light source, samples and camera.

Capturing and Processing

To account for dark current noise, we turned off the CAL1 light source and captured an image in a dark room. This image is subtracted from all images taken under each considered illuminant produced by the CAL1. All of these dark-current-noise-corrected images are flat-fielded to compensate for any variations in the light distribution on the sample plane and optical path variations between light source, sample and camera. For this, we first take an image $\mathbf{A}_B$ of a white background (see Figure 3a) and then an image $\mathbf{A}$ of the sample (see Figure 3b and 3c) under the same illuminant. The flat-fielded image $\mathbf{A}'$ is computed as follows:

$$\mathbf{A}' = \overline{\mathbf{A}_B} \frac{\mathbf{A}}{\mathbf{A}_B} \tag{2}$$

where all operations are performed pixel- and channel-wise and $\overline{\mathbf{A}_B}$ is the average of a 100×100 pixel window in the center of $\mathbf{A}_B$. Flat-fielding is performed on intensity linear images. For capturing targets of highly translucent materials, a highly non-uniform illumination might introduce measurement errors due to subsurface light transport between patches, which cannot be compensated by flat-fielding. Therefore, we ensured that the measurement area, i.e. the area covered by the target, is already very uniformly illuminated with only an irradiance-difference of approx. 10% between center and margin.

Since our light source comprises 22 LEDs, we obtain for a target 22 flat-fielded images. A homography transformation is used to correct for projective distortions caused by the 0/45 geometry. One RGB value for each patch and illuminant is extracted by averaging the RGB values of the central 20% patch-pixels to reduce the impact of noise. Such a small fraction of patch-pixels is considered to minimize color interference from neighboring patches caused by subsurface light transport within the highly translucent printing materials. For this reason, we used also a relatively large patch size of 1.75cm $\times$ 1.75cm. After this procedure, a total of 22 RGB values per patch are obtained, each corresponding to the LED illuminant under which the target was captured.

Estimating Camera Sensitivities

In order to increase the spectral variability of the stimuli, we use a Color Checker SG chart with 140 color patches. The

patch-reflectances were measured with a Barbieri Spectro LFP spectrophotometer in a circular 45/0 geometry.

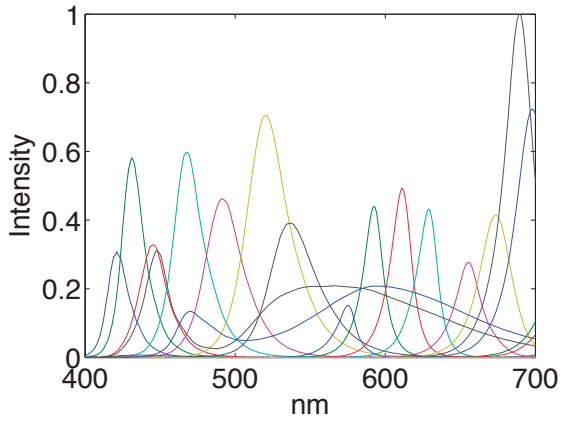

Figure 2: Normalized spectral power distributions of the 22 LED integrated into the CAL1 light source.

The spectral power distributions of the illuminants, the patch reflectances as well as the corresponding RGB values can be inserted into Equation (1) resulting in the equation system

$$\mathbf{C} = (\mathbf{C_1}, \ldots, \mathbf{C_{22}}) = \mathbf{S}\Big(D(\mathbf{i_1})\mathbf{R}, \ldots, D(\mathbf{i_{22}})\mathbf{R}\Big) + \varepsilon' = \mathbf{SR_I} + \varepsilon' \quad (3)$$

where $\mathbf{i_1}, \ldots, \mathbf{i_{22}}$ are the spectral power distributions of the LED illuminants, $\mathbf{R}$ is the matrix containing the Color Checker SG reflectances as column vectors and $\mathbf{C_j}$ is a matrix containing the RGB values as column vectors corresponding to the captured target under illuminant $\mathbf{i_j}$. This equation system can be solved with respect to the sensitivities $\mathbf{S}$. Unfortunately, such a solution is sensitive to noise as already observed by Jiang et al. [10]. Therefore, we use a principal component analysis (PCA) approach employing a-priori knowledge of the sensitivity curves. In particular, we use the sensitivity database of 28 commercial cameras from Jiang et al. [10] and compute the first four principal components for each sensitivity curve k = R, G, B describing 97% of the database's total variance. The corresponding four characteristic sensitivities are combined to a matrix $\mathbf{P}^k = (\mathbf{p}_1^k, \ldots, \mathbf{p}_4^k)^T$ and used in a four-dimensional linear model $\mathbf{s}_k = \alpha_k \mathbf{P}^k$, where $\mathbf{S} = (\mathbf{s}_R^T, \mathbf{s}_G^T, \mathbf{s}_B^T)^T$. Inserting this model into Equation (3) and solving it with respect to $\mathbf{s}_k$ in a least square sense yields

$$\mathbf{s}_k = \mathbf{C}(\mathbf{P}^k\mathbf{R_I})^T((\mathbf{P}^k\mathbf{R_I})(\mathbf{P}^k\mathbf{R_I})^T)^{-1}\mathbf{P}^k, \quad k = R, G, B. \quad (4)$$

The estimated sensitivities are shown in Figure 4.

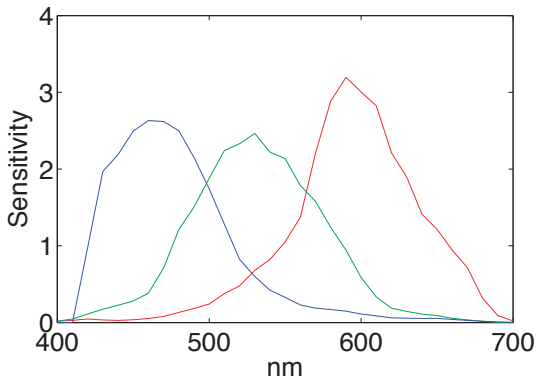

Figure 4: Estimated sensitivities for the Canon 5D Mark III camera.

Estimating Spectral Reflectances

With the estimated camera sensitivities $\mathbf{S}$ and the internally-measured spectral power distribution $\mathbf{i_1}, \ldots, \mathbf{i_{22}}$ of the LEDs, we can estimate spectral reflectances of a 3D printed target from its captured RGB values. For this, we use Wiener estimation

$$\mathbf{r} = \mathbf{KF}^T(\mathbf{FKF}^T + \mathbf{K}_\varepsilon)^{-1}\mathbf{c_r}, \quad (5)$$

where $\mathbf{r}$ is the estimated reflectance, $\mathbf{K}$ is the reflectance covariance matrix, $\mathbf{F} = (D(\mathbf{i_1})\mathbf{S}^T, \ldots, D(\mathbf{i_{22}})\mathbf{S}^T)^T$ is the $66 \times n$ dimensional combined lighting matrix of the system, $\mathbf{K}_\varepsilon$ is the noise covariance matrix and $\mathbf{c_r} = (\mathbf{c_1}^T, \ldots, \mathbf{c_{22}}^T)^T$ is the 66-dimensional vector of dark-current-noise-corrected and flat-fielded RGB camera responses captured under the 22 LEDs. The reflectance covariance matrix $\mathbf{K}$ is computed using reflectances of the 140 color patches of the Color Checker SG. The noise covariance matrix is computed for each patch independently as follows

$$\begin{aligned} \mathbf{K}_\varepsilon &= D(\boldsymbol{\sigma}^2), \quad (6) \\ \boldsymbol{\sigma}^2 &= \left(\sigma_{1R}{}^2, \sigma_{1G}{}^2, \sigma_{1B}{}^2, \ldots, \sigma_{22R}{}^2, \sigma_{22G}{}^2, \sigma_{22B}{}^2\right), \end{aligned}$$

where D is defined as in Equation (1) and σ_{jk} is the standard deviation for channel k under illuminant $\mathbf{i_j}$ computed for the central 20% of the pixels within the patch. The standard deviations are determined on the dark-current-noise-corrected and flat-fielded RGB camera responses. This patch-wise noise-variance computation dramatically improves the reconstruction results.

Note that a white reference patch does not need to be captured for canceling out the illuminant from the reflectance estimation.

Results and Discussion

In this section, we are evaluating the spectral and colorimetric accuracy of the setup. The accuracy of the estimated reflectances depends on the accuracy of the estimated camera sensitivities employed by the Wiener method. Since we do not have the ground truth sensitivities, we analyze the RGB deviations between captured RGBs and RGBs predicted by Equation (1) for known stimuli.

Evaluating Camera Sensitivities

To evaluate the accuracy of the estimated sensitivities we use stimuli obtained by capturing the Color Checker SG target under

(a) Capturing the white board

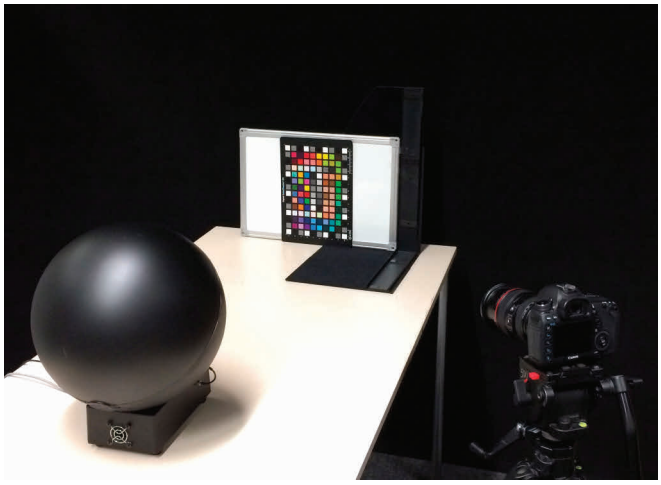

(b) Capturing the Color Checker SG

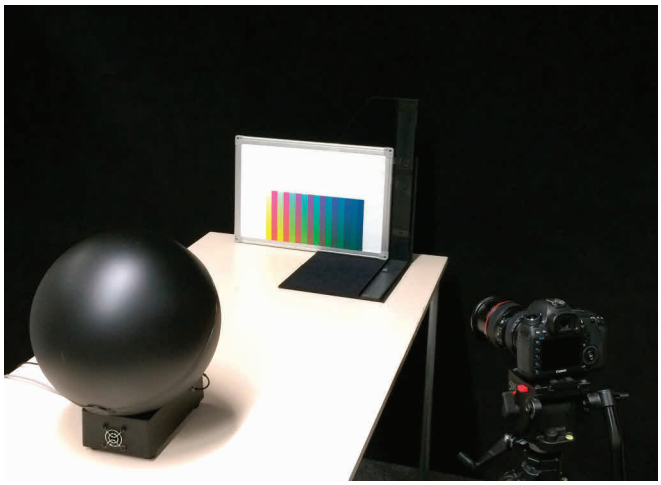

(c) Capturing the printed target

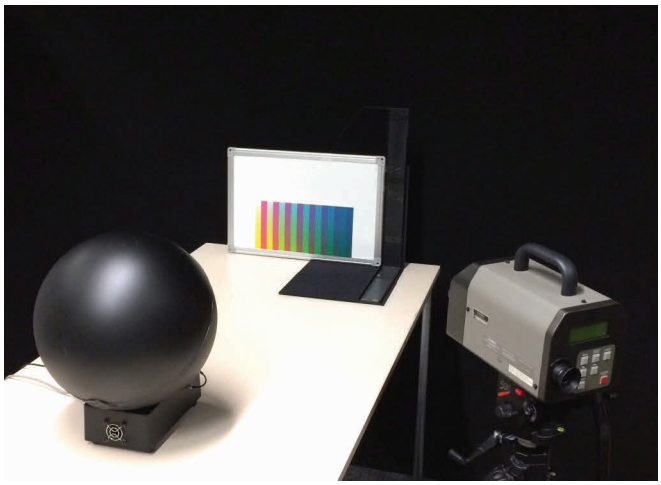

(d) Verification with a Spectroradiometer

Figure 3: Measurement setups. The black sphere is the CAL1 light source.

all LED illuminants provided by the CAL1 light source. This results in 3080 captured RGB values which are compared with the RGB values predicted by Equation (1). The absolute difference between captured and predicted R,G,B values for each channel as well as the root-mean-square errors considering all three channels are shown in Figure 5, where the 16-bit encoded channel values obtained by the camera are normalized to 1. The average root-mean-square RGB error is approx. 0.24% and the maximum error is 3.05%. Table 1 shows the error statistics. These errors are very small and validate the high accuracy of the estimated spectral sensitivities.

Channel	Mean	Maximum	95^{th} percentile
Red	0.0026	0.0326	0.0108
Green	0.0024	0.0332	0.0112
Blue	0.0021	0.0252	0.0097
RGB	0.0024	0.0305	0.0106

Table 1: **Prediction performance of Equation** (1) **incorporating the estimated camera sensitivities for 3080 training stimuli.**

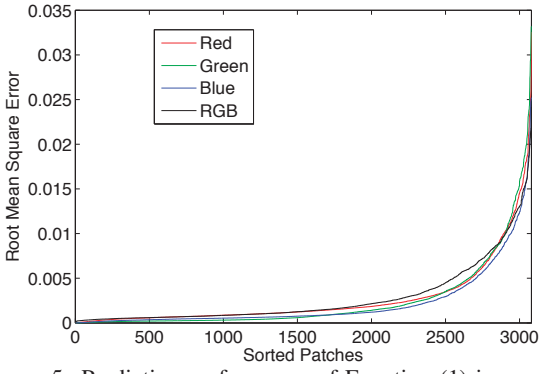

Figure 5: Prediction performance of Equation (1) incorporating the estimated camera sensitivities for 3080 training stimuli.

Evaluating Reflectance Estimation

As shown by Arikan et al. [1] spectrophotometers used in the graphic arts industry cannot accurately measure highly translucent materials. Therefore, we use the Konica-Minolta CS1000 spectroradiometer and a white patch with known reflectance to

obtain reference measurements employing the same 0/45 measurement geometry. We adjusted the CAL1 light source to simulate the CIED50 illuminant and measured the light $\mathbf{p_w}$ reflected by the Color Checker's white patch with known reflectance $\mathbf{r_w}$. Then, we placed the 3D printed patch exactly at the same position as the Color Checker's white patch and measured the light reflected from the central part of the patch (roughly 20 percent of the area). From these quantities the patch's reflectance can be computed as follows:

$$\mathbf{r_m} = \frac{\mathbf{p_m} \cdot \mathbf{r_w}}{\mathbf{p_w}}, \tag{7}$$

where the computation is performed wavelength-wise.

We used the eight Neugebauer primaries of the Objet 500 Connex3 printer employing standard white, cyan and magenta resins and using a yellow colored support resin. Patches are printed as described by Brunton et al. [2]. Measured and estimated reflectances for the Neugebauer primaries are compared in Figure 6. Table 2 shows the spectral root-mean-square errors and the CIEDE2000 errors under illuminant CIED50. The deviations are within the inter-instrument variability – up to mean 2.6 / max. 5.51 CIE76 units for BCRA tiles – reported for hand-held spectrophotometers used in graphic arts [24]. Thus, the estimated reflectances should have sufficient accuracy to be used for spectral printer modeling. One drawback of our setup is a missing LED emitting at 400nm as shown in Figure 2. This is the reason why the largest spectral deviations can be observed for this wavelength.

(C,M,Y)	CIEDE2000 [CIED50]	Spectral RMS
(0,0,0)	0.29	0.0238
(1,0,0)	0.39	0.0414
(0,0,1)	0.58	0.0267
(1,0,1)	1.10	0.0314
(0,1,0)	0.36	0.0293
(1,1,0)	0.50	0.0243
(0,1,1)	0.12	0.0299
(1,1,1)	2.01	0.0225
average	0.67	0.0286

Table 2: **Spectral and colorimetric deviations between spectroradiometric measurements and estimated reflectances for the Neugebauer primaries.**

Conclusion

In this work, we presented a spectral acquisition system employing a LED-based spectrally-tunable light source and a trichromatic camera for the purpose of accurately measuring reflectance spectra of highly translucent 3D printing materials. As shown by Arikan et al. [1], spectrophotometers used in the graphic arts industry cannot be used because their measurements are systematically biased towards lower reflectance for such materials. The proposed setup is designed to avoid this bias by using a very uniform illumination of the whole target. It shall be integrated in a gonio-imager to sample the Bidirectional Reflectance Distribution Function (BRDF) of 3D printed samples by densely capturing colorimetric data for one adjusted illuminant (e.g. CIED50) and sparse spectral measurements that can be used as additional information to reconstruct reflectances from the colorimetric samples. In this work, the characterization of the system and the spectral accuracy was evaluated for a 0/45 measurement geometry.

In the characterization step, we used the tunable light source and *a priori* knowledge of spectral sensitivities to determine the camera sensitivities. Inserting these sensitivities into the linear image formation model, results in average root-mean-square RGB errors of 0.24% and maximum errors of 3%. For reflectance reconstruction, we captured the printed target under all LEDs included in the spectrally-tuneable light source and used the estimated sensitivities, the spectral power distribution of the illuminant (recorded by a spectroradiometer included in the light source) and the acquired RGB data. Reflectance were estimated by the Wiener method for which a patch-wise noise-covariance matrix was computed. Capturing a white reference to normalize reflectances is not required. Average spectral root-mean-square deviations to spectroradiometric measurements are 0.0286 for the Neugebauer primaries or 0.67 CIEDE2000 units considering illuminant CIED50. These deviations are within the inter-instrument-variability of hand-held instruments used in graphic arts. The accuracy of the reflectance estimates should be sufficient for the purpose of spectrally modeling multi-material polyjet 3D printers.

References

[1] Can Ates Arikan, Alan Brunton, Tejas Madan Tanksale, and Philipp Urban. Color-managed 3d printing with highly translucent printing materials. In *IS&T/SPIE Electronic Imaging*, pages 93980S–93980S. International Society for Optics and Photonics, 2015.

[2] A. Brunton, C. A. Arikan, and P. Urban. Pushing the limits of 3d color printing: Error diffusion with translucent materials. *ACM Transactions on Graphics*, 2015 (accepted - preprint on `http://arxiv.org/pdf/1506.02400.pdf`).

[3] V. Cheung, S. Westland, C. Li, J. Hardeberg, and D. Connah. Characterization of trichromatic color cameras by using a new multispectral imaging technique. *Journal of the Optical Society of America A*, 22(7):1231–1240, 2005.

[4] J. M. DiCarlo and B. A. Wandell. Spectral estimation theory: beyond linear but before Bayesian. *Journal of the Optical Society of America A*, 20(7):1261–1270, 2003.

[5] M. Ebner. Estimating the spectral sensitivity of a digital sensor using calibration targets. In *Proceedings of the 9th annual conference on Genetic and evolutionary computation*, pages 642–649. ACM, 2007.

[6] T. Eckhard, E. M. Valero, J. Hernández-Andrés, and V. Heikkinen. Evaluating logarithmic kernel for spectral reflectance estimation – effects on model parametrization, training set size, and number of sensor spectral channels. *JOSA A*, 31(3):541–549, 2014.

[7] G. D. Finlayson, S. Hordley, and P. M. Hubel. Recovering device sensitivities with quadratic programming. In *IS&T/SID*, pages 90–95, Scottsdale Ariz., 1998.

[8] C. Godau and P. Urban. Spatio-spectral image restoration. In *Color and Imaging Conference*, volume 2013, pages 27–32. Society for Imaging Science and Technology, 2013.

[9] Shuai Han, Yasuyuki Matsushita, Imari Sato, Takahiro Okabe, and Yoichi Sato. Camera spectral sensitivity estimation from a single image under unknown illumination by using fluorescence. In *Computer Vision and Pattern Recognition (CVPR), 2012 IEEE Conference on*, pages 805–812. IEEE,

2012.

[10] Jun Jiang, Dengyu Liu, Jinwei Gu, and Sabine Susstrunk. What is the space of spectral sensitivity functions for digital color cameras? In *Applications of Computer Vision (WACV), 2013 IEEE Workshop on*, pages 168–179. IEEE, 2013.

[11] F. König. *Die Charakterisierung von Farbsensoren*. PhD thesis, Rheinisch-Westfälische Technische Hochschule Aachen, Germany, 2001.

[12] C. Li and M. R. Luo. The estimation of spectral reflectances using the smoothness constraint condition. In *IS&T/SID, 9th Color Imaging Conference*, pages 62–67, Scottsdale Ariz., 2001.

[13] L. T. Maloney and B. A. Wandell. Color constancy- A method for recovering surface spectral reflectance. *Optical Society of America, Journal, A: Optics and Image Science*, 3:29–33, 1986.

[14] P. Morovic and G. D. Finlayson. Metamer-set-based approach to estimating surface reflectance from camera RGB. *Journal of the Optical Society of America A*, 23(8):1814–1822, 2006.

[15] Y. Murakami, K. Fukura, M. Yamaguchi, and N. Ohyama. Color reproduction from low-SNR multispectral images using spatio-spectral Wiener estimation. *Optics Express*, 16(6):4106–4120, 2008.

[16] Y. Murakami, K. Ietomi, M. Yamaguchi, and N. Ohyama. Maximum a posteriori estimation of spectral reflectance from color image and multipoint spectral measurements. *Applied Optics*, 46(28):7068–7082, 2007.

[17] Y. Murakami, M. Yamaguchi, and N. Ohyama. Piecewise wiener estimation for reconstruction of spectral reflectance image by multipoint spectral measurements. *Applied optics*, 48(11):2188–2202, 2009.

[18] Junichi Nakamura. *Image sensors and signal processing for digital still cameras*. CRC press, 2005.

[19] G. Sharma and H. J. Trussell. Characterization of scanner sensitivity. In *IS&T/SID*, pages 103–107, Scottsdale Ariz., 1993.

[20] G. Sharma and H. J. Trussell. Set theoretic estimation in color scanner characterization. *Journal of Electronic Imaging*, 5:479–489, 1996.

[21] Norimichi Tsumura, Yoichi Miyake, and Vladimir Bochko. Spectral color imaging system for estimating spectral reflectance of paint. *Journal of Imaging Science and Technology*, 51(1):70–78, 2007.

[22] P. Urban, M. R. Rosen, and R. S. Berns. Spectral Image Reconstruction using an Edge Preserving Spatio-Spectral Wiener Estimation. *Journal of the Optical Society of America A*, 26(8):1868–1878, 2009.

[23] Philipp Urban, Michael Desch, Kathrin Happel, and Dieter Spiehl. Recovering camera sensitivities using target-based reflectances captured under multiple led-illuminations. In *Proc. of Workshop on Color Image Processing*, pages 9–16, 2010.

[24] D. R. Wyble and D. C. Rich. Evaluation of methods for verifying the performance of color-measuring instruments. part ii: Inter-instrument reproducibility. *Color Research & Application*, 32(3):176–194, 2007.

[25] X. Zhang and H. Xu. Reconstructing spectral reflectance by dividing spectral space and extending the principal components in principal component analysis. *Journal of the Optical Society of America A*, 25(2):371–378, 2008.

[26] Hongxun Zhao, Rei Kawakami, Robby T Tan, and Katsushi Ikeuchi. Estimating basis functions for spectral sensitivity of digital cameras. In *Meeting on Image Recognition and Understanding*, volume 2009, 2009.

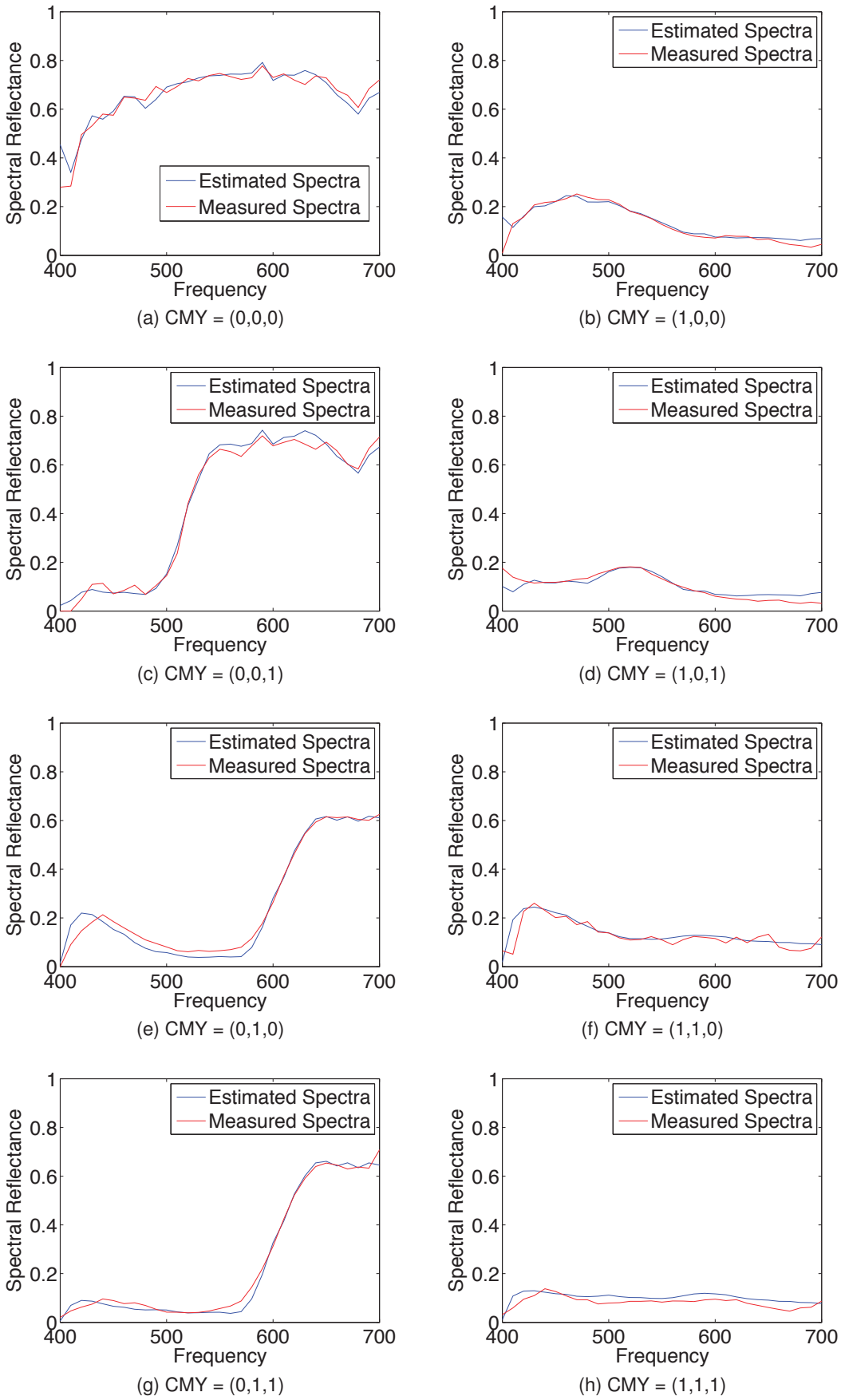

Figure 6: Comparison between estimated and measured spectra.